PHYSICAL REVIEW A VOLUME 36, NUMBER 2 JULY 15, 1987

Postponement of Hopf bifurcations by multiplicative colored noise

L. Fronzoni
Dipartimento di Fisica, Università di Pisa, Piazza Torricelli 2, 56100 Pisa, Italy

R. Mannella, P. V. E. McClintock, and Frank Moss*
Department of Physics, University of Lancaster, Lancaster LA1 4YB, United Kingdom
(Received 12 January 1987)

Problems related to the definition of a Hopf bifurcation in the presence of noise are discussed in terms of three physical observables: the correlation functions, the power spectra, and the statistical densities. Of these, only the statistical density exhibits a distinct noise-induced transition. For a specific definition, only postponements are observed in analog simulator experiments with a Brusselator subject to white and colored noise on the control parameter. A recent prediction due to Lefever and Turner [Phys. Rev. Lett. **56**, 1631 (1986)] is qualitatively tested.

I. INTRODUCTION

One of the more striking effects of parametric (multiplicative) noise on nonlinear dynamical systems which exhibit instabilities is to induce a shift in the critical mean value of the control parameter which drives the instability. Such shifts were first observed in Fokker-Planck models of white-noise-driven systems with applications in biology[1] and chemical dynamics,[2] but were soon applied to various systems,[3–5] including general bistability.[6] Early applications were to turbulence transitions in nematic liquid crystals[3,4,7] and superfluid helium.[8] Noise-induced shifts were originally observed in experiments on electronic oscillators[9] which were later followed by demonstrations with analog simulators which offered quantitative results in excellent agreement with the predictions of the white-noise Fokker-Planck models.[10] Early experiments with an electrohydrodynamic instability in nematic liquid crystals[11,12] have more recently resulted in beautiful and unambiguous demonstrations of noise-induced shifts,[13] as well as other effects[14] associated with the formation of dissipative structures in nonequilibrium systems. A recent theoretical assessment and review has been given.[15]

The shifts can be either toward smaller mean control-parameter values (advancements) or larger values (postponements), depending on the type of multiplicative noise, whether linear[3,6,7] or quadratic,[4] Gaussian[3–8] or dichotomous,[15] or white (most early works) or colored.[15,16] To date, to the best of our knowledge, only postponements have been observed in experiments and in analog simulations. Similar effects for harmonically modulated parameters in hydrodynamic models have been predicted[16] but not observed in experiments.[17] Postponements of the first bifurcations of discrete maps included by multiplicative noise have also been predicted and observed in numerical experiments.[18]

The shifts discussed here in systems which already deterministically exhibit a dynamical instability are one type of noise-induced transition treated by Horsthemke and Lefever,[19] the other being the so-called "pure" noise-induced transition wherein bi- or multimodality is induced by noise in a system which deterministically has either no instability or a fewer number of instabilities.[19,20]

It also should be noted that the shifts we focus on here must be distinguished from the postponements induced in bifurcating systems by deterministically sweeping a control parameter at a non-negligible velocity. Such systems, both continuous[21,22] and discrete[23,24] have recently been studied with additive noise.

In this paper we study noise-induced postponements of a critical feature of the statistical densities of noisy limit cycles using an analog electronic circuit model of the Brusselator.[25] The motivation for this work was provided by a recent theory due to Lefever and Turner[26] (LT), which predicts either advancements or postponements depending on the magnitude of the noise correlation time relative to the rotation time of the limit cycle. Only postponements are predicted in other approaches[27,28] based on normal forms.[29]

In Sec. II we discuss the (not insignificant) problem of how a Hopf bifurcation can be defined in the presence of multiplicative noise. We present, and subsequently use, a definition which is physically reasonable and, in addition, has the advantage of being easily accessible in an experiment. Section III describes our circuit model of the Brusselator and presents some examples of measured, three-dimensional statistical densities which are the raw data. In Sec. IV the data on postponements are shown. In Sec. V an algorithm is presented for transforming the measured densities into the phase space of polar coordinates used by LT, and our search for the predicted advancements is discussed. Finally, a brief discussion and conclusions are given in Sec. VI.

Our results can be summarized as follows: Using the definition presented in Sec. II, we observe only postponements for both quasiwhite and colored noise. In the transformed coordinates we observe some qualitative features predicted by LT; however, the magnitudes of the predicted advancements are too small to observe in this experiment.

II. THE HOPF BIFURCATION IN THE PRESENCE OF NOISE

The Brusselator system is defined by

$$\dot{x} = A - (1+B)x + x^2 y \ , \tag{1a}$$

$$\dot{y} = Bx - x^2 y \ , \tag{1b}$$

where A is a constant and B is the control parameter. Without loss of generality, we take $A=1$. The steady states of (1) are then $x_s = A = 1$ and $y_s = B/A = B$. The deterministic bifurcation from the fixed points $x=1$, $y=B$ for $B < B_c$ to a limit cycle occurs at the critical value $B_c = 1 + A^2 = 2$. A sample, deterministic limit cycle measured on the analog system described in Sec. III is shown in Fig. 1(a) for $B=2.5$, where $x(t)$ is plotted versus $y(t)$ on an oscilloscope screen.

FIG. 1. Limit cycles y vs x of the electronic Brusselator. (a) for $B=2.5$ without external noise; (b) for $B=2.5$, $D=0.01$, and $\tau=0.10$, plotted on the same scale as (a); and (c) $B=1.8$ ($<B_c$), $D=0.01$, and $\tau=1.0$. The scale is expanded by a factor of 2.5 compared to (a) and (b). The dot at the center is the fixed point observed without external noise.

In this work we investigate the effects of multiplicative noise on the control parameter, that is, we let $B \to B(t) = \langle B \rangle + V_n(t)$, where V_n is a colored noise defined by $\langle V_n \rangle = 0$, and

$$\langle V_n(t) V_n(s) \rangle = (D/\tau) e^{-|t-s|/\tau} \ . \tag{2}$$

The noise intensity is D, and its correlation time is τ. The limit cycle of Fig. 1(a) now becomes noisy, as shown in Fig. 1(b), and in order to proceed further it is necessary to measure some statistical quantity, for example, the power spectra, correlation functions, or the statistical densities.

We are interested in the effects of the noise on the location of the bifurcation. It therefore becomes necessary to precisely define what is meant by a Hopf bifurcation in the presence of noise. Defining the deterministic bifurcation in our case presents no problem: It is the perfectly articulated transition from the time-independent state for $B < B_c$ to the oscillatory limit cycle precisely at $B = B_c$. However, the difficulties with attempts to adapt this definition to the noisy case are illustrated in Fig. 1(c). Here the same noise intensity obtains as in Fig. 1(b), but now $B = 1.8 < B_c$. Limit-cycle-like behavior, though at reduced amplitude and stochastic in nature, is clearly evident. This photograph is a double exposure, with the noise momentarily removed to reveal the time-independent state which shows as the bright spot in the center of the trajectories.

Figure 1(c) suggests that when noise is present, even very small noise, there is always harmonic behavior, also for $B \ll B_c$, so that the bifurcation is difficult to define. In order to further test this assertion, we show in Fig. 2 a series of measured autocorrelation functions and power spectra for $D=0.01$ (quite a small value) and for B ranging from $B > B_c$ to $B \ll B_c$. All show the clear signature of harmonic behavior at the Brusselator limit-cycle frequency, except Fig. 2(e) where the power spectrum shows no clearly resolved peak at $\omega > 0$; however, even for this very small value of $B=0.60$, the correlation function shows damped harmonic behavior with the first maximum still located at ω_B^{-1}. [All plots in Fig. 2 were made to the same horizontal scale so that the locations of ω_B^{-1} and ω_B are the same in 2(a)–2(e)]. This problem has been studied in detail by Wiesenfeld who examined period doubling and Hopf bifurcations in the presence of *additive* noise.[30–32] He has observed the same persistence of harmonic behavior for $B < B_c$ which he has called the "noisy precursor" of the actual bifurcation.

An early and excellent discussion of transitions to limit-cycle behavior in the presence of noise has been given by San Miguel and Chaturvedi,[33] based on the idea of an irreversible circulation of fluctuations.[34] These authors stress that limit-cycle behavior cannot be defined from the stationary probability density alone, but instead they define an order parameter based on the circulation $\langle L_{xy} \rangle = \langle x\dot{y} - y\dot{x} \rangle$. It is easy to imagine single-peaked, stationary densities, and those with crater or craterlike shapes for which this flow could be evaluated. As shown below, however, our measured densities display three distinct shapes, single peaked, craterlike but with an open rim, and finally cratered with a closed rim, which develop

successively as B is increased and/or D is decreased (for $B > B_c$).

Lacking distinct transitions in the correlation functions or the power spectra which could mark the occurrence of a bifurcation, and absent a single transition from a single-peaked density through which all cross sections perpendicular to the xy plane are monomodal to one with a *closed* crater, we have examined instead the topology of the two-dimensional, stationary statistical densities $P(x,y)$. For small noise intensity D, and for $B > B_c$, these are shaped like a crater. As D is increased, or B is decreased, the crater floor rises until at some critical value D^*, which occurs also at a critical mean value of the bifurcation parameter B^*, the floor attains the same altitude as the lowest surrounding ridge. In other words, the critical density is that one which divides the class of those densities for which at least one cross section through $P(xy)$ and parallel to the xy plane, is doubly connected from the class of those which have only singly connected cross sections. Specifically we define the pairs D^* and B^* as those values at which $P(x,y)$ is the critical one. This definition is taken in the spirit of the noise-induced transitions of

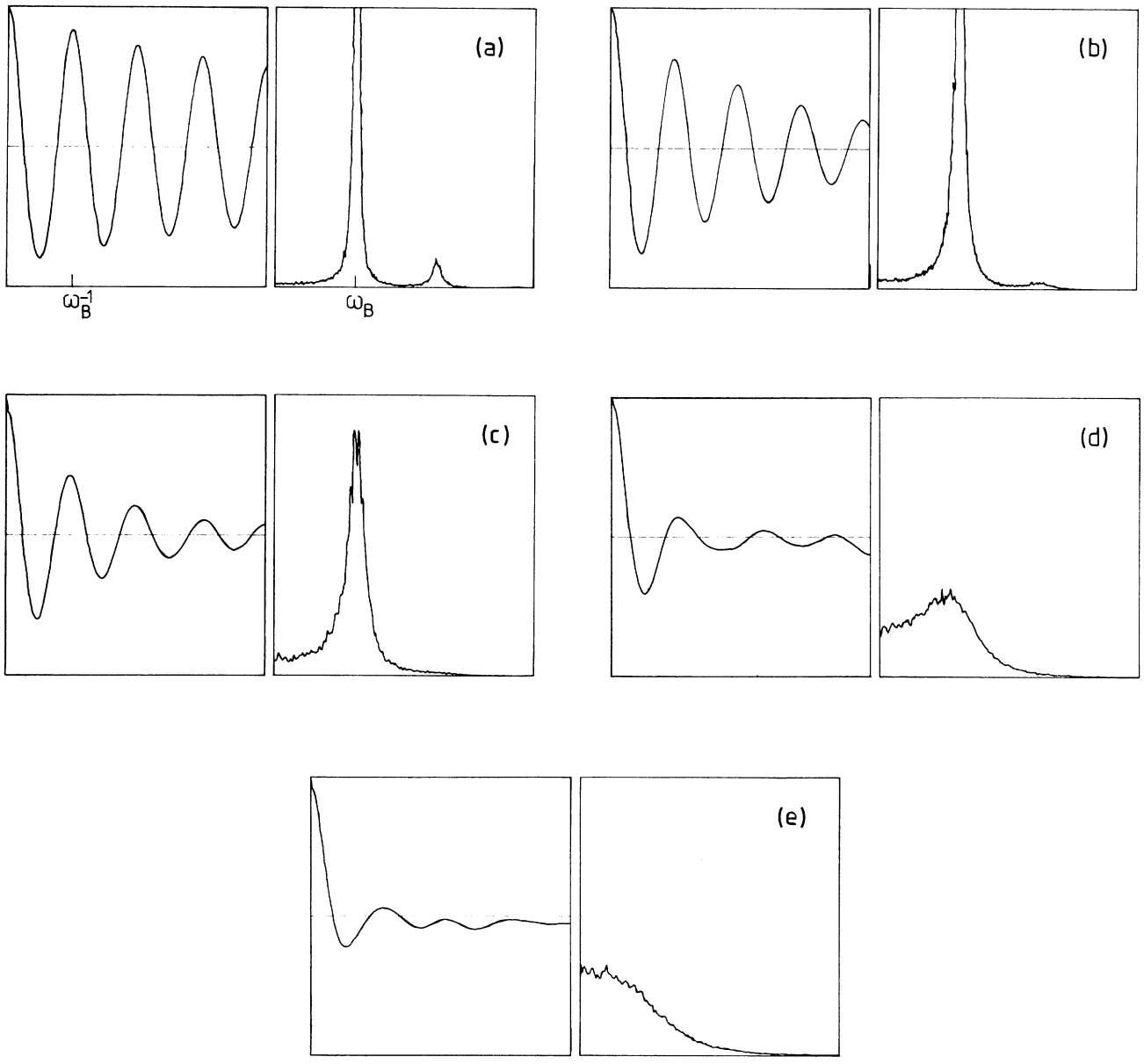

FIG. 2. Autocorrelation functions $\langle x(t)x(s)\rangle$, shown on the left, and power spectra of $x(t)$ on the right for $D=0.01$ and $\tau=1.0$. (a) $B=2.20$, (b) $B=2.00$, (c) $B=1.80$, (d) $B=1.20$, (e) $B=0.60$. The Brusselator period ω_B^{-1} and frequency ω_B, measured in the absence of noise are marked on the horizontal axes of (a). All plots (a)–(e) are produced on the same horizontal scale, so the locations of these two quantities are identical.

Horsthemke and Lefever.[19] In the Appendix we discuss the San Miguel-Chaturvedi order parameter applied to the Brusselator, and show that a suitably generalized version of it becomes nonzero at exactly the critical density defined here. In Sec. III the electronic Brusselator is described, and some examples of measured densities $P(x,y)$ are shown.

III. THE ELECTRONIC CIRCUIT MODEL

The electronic circuit model of Eqs. (1) is shown schematically in Fig. 3. This is an example of the "minimum-component" design used at the University of Pisa which employs only two multipliers, two operational amplifiers, and one inverter (amplifier with gain equal to -1). The operation can be understood by writing two equations for the outputs of the two amplifiers $V_1 \equiv y$ and $V_4 = x$:

$$(dx/dt')RC = V_0 - [1 + (B + V_n)]x + x^2 y \ , \tag{3a}$$

$$(dy/dt')RC = (B + V_n)x - x^2 y \ , \tag{3b}$$

where the limit-cycle frequency is established by the two identical time constants $\omega_B = 1/RC$, and where $V_0 \equiv A = 1$ V. Note also that Eqs. (3) can be written in the form of Eqs. (1) by substituting the dimensionless time $t \equiv t'/RC$ for the real time t'. This time t also appears in Eq. (2) if we define the dimensionless noise correlation time $\tau = \tau_n/RC$, where τ_n is the actual noise correlation time determined by the linear filter at the output of the wide-band noise generator. Throughout this experiment $RC = 10^{-4}$ s. The values of τ_n varied from 10^{-5} s ($\tau = 0.1$, quasiwhite noise) to 10^{-3} s ($\tau = 10$, very colored noise). The noise voltage V_n is accurately Gaussian with zero mean. The noise intensity D was obtained from measured values of $\langle V_n^2 \rangle \equiv D/\tau$ at the output of the filter.

In operation, the voltages x and y were connected to a data-analysis system (Nicolet Lab-80 or 1180) which first digitized time series of $x(t)$ and $y(t)$, then computed a first approximation to $P(x,y)$. Successive time series were obtained and a running average of $P(x,y)$ was accumulated until satisfactorily small statistical errors were evident. Typically 1 to 5 million points in the time series of each variable were used. A sample measured density, for $B > B^*$ and for $D < D^*$ for noise of moderate intensity, is shown in Fig. 4, with a three-dimensional view depicted

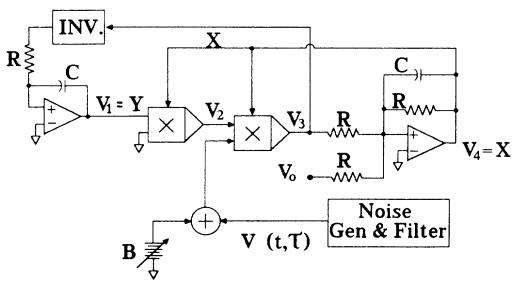

FIG. 3. The electronic Brusselator. The multipliers, shown by crosses, are Analog Devices AD 534. The output of the first multiplier is $V_2 = xy$. The output of the second is $V_3 = x^2 y - (B + V_n)x$. The other voltages are defined in the text.

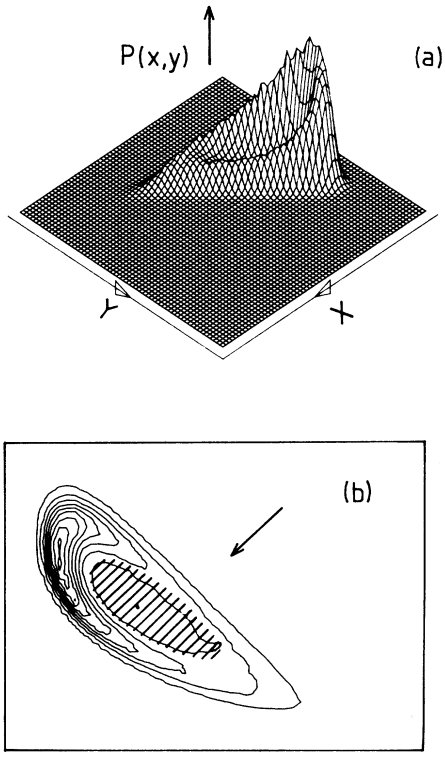

FIG. 4. Measured $P(x,y)$ for $B = 2.2$, $D = 0.008$, and $\tau = 0.10$. (a) a three-dimensional view as observed from the direction indicated by the arrow in (b). (b) a plot of nine contours of constant probability at equally spaced intervals. The cross-hatched area indicates the crater which is concave downward.

in 4(a) and its contour plot shown in 4(b). The arrow in Fig. 4(b) shows the direction in which Fig. 4(a) is viewed. The crater is clearly visible in both plots, and is indicated by the cross hatching in 4(b).

IV. THE RESULTS

Figure 5(a) shows a measured density which is approximately critical, i.e., for which $D \simeq D^*$ and $B \simeq B^*$. In practice, this condition was determined by observing the contours, and vertical cross sections cut parallel to the x axis. Figure 5(b) shows a density for $D > D^*$. Normally, D was set at a desired value and B was adjusted by trial and error until the approximately critical density was found. We always found that for $D > 0$, $B^* > B_c$, i.e., we always found postponements.

The largest postponements (for a given D) were found for quasiwhite noise. Our results for several noise correlation times are shown in Fig. 6 in the form of a phase diagram, where in the regions above and to the left of a line joining the data for a given τ the densities are cratered with a doubly connected horizontal cross section, while below and to the right, they are not. The straight lines serve only as a guide to the eye, but suggest a linear relation between the magnitude of the postponement and the noise intensity. In Fig. 7 we have replotted the same

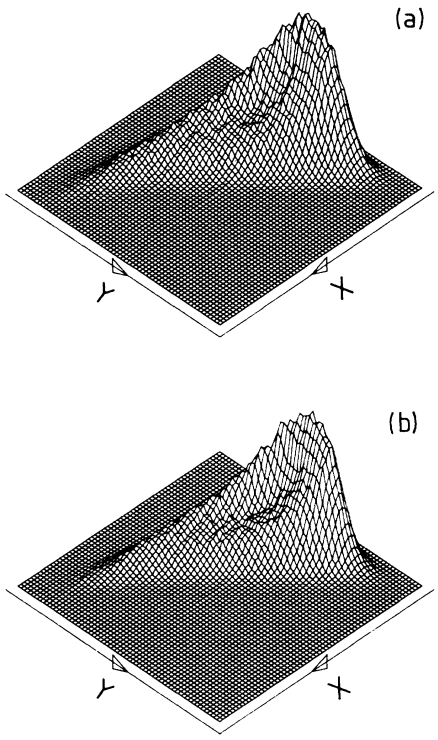

FIG. 5. Measured $P(x,y)$ for $B=2.2$ and $\tau=0.10$. (a) $D\simeq D^*=0.016$ (and $B\simeq B^*$). (b) $D=0.03>D^*$ (and $B<B^*$).

data, except now B^* is displayed versus τ on a semilog plot. The solid lines suggest an exponential relation, though we have not included data for the smallest τ and D.

V. THE SEARCH FOR ADVANCEMENTS

For quasiwhite noise, specifically for $\tau_n \ll \omega_B^{-1}$, LT predict advancements. They show that near the bifurcation

$$\omega_B^{-1} = |\langle B\rangle - B_c|^{-1} = \epsilon^{-2} . \tag{4}$$

With $A=1$, the transformation equations which define the polar coordinates shown in Fig. 8 become[26]

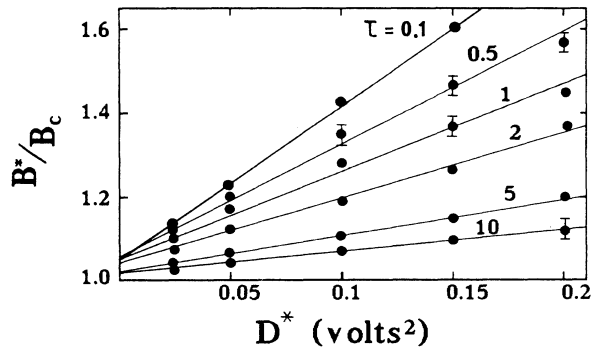

FIG. 6. The postponed bifurcation parameter B^* vs noise intensity D^* for various noise correlation times.

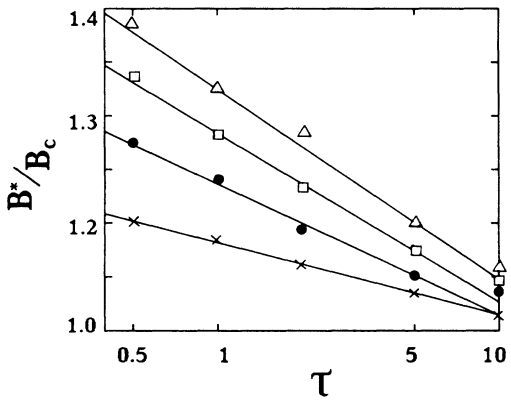

FIG. 7. B^* vs τ for $D^*=0.2$ (triangles), 0.15 (squares), 0.10 (circles), and 0.05 (crosses).

$$x = 1+\epsilon u^{1/2}\cos\theta , \tag{5a}$$

$$y = 2+I\epsilon^2+\epsilon u^{1/2}(\sin\theta-\cos\theta) , \tag{5b}$$

where $I=1,0,-1$ for B above, at, or below B_c. Examples of Eqs. (5) are plotted in Fig. 8 where it is clear that u determines the size of the limit cycle. LT then developed a colored-noise Fokker-Planck analysis from which they are able to calculate the two-dimensional stationary densities $P(u,\theta)$. After integrating over θ they arrive at a one-dimensional density $P(u)$, and from $\partial_u P(u)=0$ they obtain the location of its extremum u_m. Their final formula is

$$u_m = \tfrac{4}{3}+\epsilon^2(-\tfrac{352}{81}+47\langle V_n^2\rangle/36) . \tag{6}$$

As the negative sign indicates, for small enough noise, in-

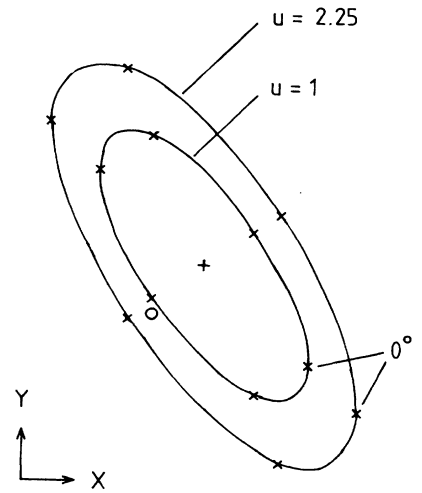

FIG. 8. The idealized limit cycle of Eqs. (5), used by LT to calculate $P(u,\theta)$. This plot is for $x=x_0+\epsilon u^{1/2}\cos\theta$ and $y=y_0+\epsilon^2+\epsilon u^{1/2}(\sin\theta-\cos\theta)$, with $x_0=0.1$ and $y_0=0.1$. The crosses mark the locations of successive values of θ in increments of $\pi/3$.

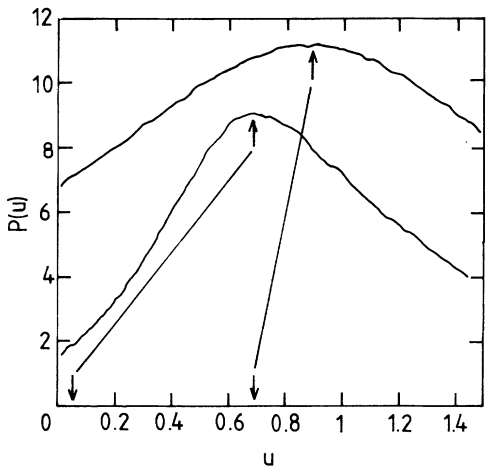

FIG. 9. One-dimensional densities in the polar coordinate u, for $\langle V_n^2 \rangle = 0.05$. The broad density is for $B = 2.15$ and the narrow one is for $B = 2.30$. The arrows on the u axis show the locations of the maxima u_m predicted by Eq. (6).

creasing ϵ^2 from small values should move the location of the maximum toward smaller values. Alternatively, one can fix ϵ^2 and increase $\langle V_n^2 \rangle$ which moves u_m toward larger values indicating that the "mean amplitude" of the limit cycle is increased, indicating an advancement.

We have measured several two-dimensional densities $P(x,y)$ for $\tau = 0.1$, then transformed them to $P(u,\theta)$ using Eqs. (5), and subsequently summed over θ, in order to obtain $P(u)$. First, we fixed $D = 0.01$ (or $\langle V_n^2 \rangle = 0.005$) (Ref. 35) and varied $\langle B \rangle$. Two such densities, one for $\langle B \rangle = 2.15$ (or $\epsilon = 0.15$) and the other for $\langle B \rangle = 2.30$ (or $\epsilon = 0.30$) are shown in Fig. 9. There is at least qualitative agreement with the prediction of LT, since the observed leftward shift of u_m with increasing ϵ^2 for small noise intensity is a certain indication of the negative sign in Eq. (6). The formula predicts, however, a considerably larger shift than we observe. This may be because either the experimental $\epsilon^2 = 0.30$ or $\tau = 0.1$ are too large (or both). The theory is valid only for small ϵ, and very small τ.

We have used the same procedure in attempts to observe shifts in u_m with fixed ϵ^2 and variable $\langle V_n^2 \rangle$. The results are summarized in Table I. Note that u_m is a measure of the effective size of the limit cycle. That u_m increases with increasing $\langle V_n^2 \rangle$ for small enough τ is an important prediction of the LT theory.

No statistically significant shifts were observed as shown by the two representative errors. The entries calculated from Eq. (6) indicate only a very weak dependence on $\langle V_n^2 \rangle$. In an effort to enhance the shifts we have tried larger values of both ϵ^2 and $\langle V_n^2 \rangle$. Unfortunately, they lead to much broader densities $P(u)$ and hence to larger error bars in u_m^{expt}, so that the search was again inconclusive.

TABLE I. Calculated and measured maxima in the density $P(u)$ for $\epsilon^2 = 0.10$.

$\langle V_n^2 \rangle$	u_m^{expt}	u_m^{theor}
0.02	0.69±0.05	0.47
0.04	0.63	0.47
0.05	0.62	0.48
0.08	0.69	0.48
0.10	0.71±0.08	0.49
0.15	0.75	0.50

VI. CONCLUSIONS

We have studied a Hopf bifurcation from a time-independent state to a limit cycle with noise on the bifurcation parameter using an electronic model of the Brusselator. Measurements of the power spectra and autocorrelation functions of the fluctuating output show evidence of harmonic behavior and no critical features for all mean values of the bifurcation parameter. However, a critical feature of the measured two-dimensional densities can be defined in terms of its topology. Using this definition, substantial postponements of the mean critical bifurcation parameter are found for both long and short noise correlation times. However, the question of whether or not the effective size of the limit cycle increases with increasing D for small τ (which in the LT theory would be the signature of an advancement) remains open, since the predicted increases were to small to measure in this experiment.

ACKNOWLEDGMENTS

We are grateful to R. Lefever for suggesting this work and for a number of stimulating discussions. We are also indebted to K. Wiesenfeld for a valuable correspondence and for sending us copies of his papers on noisy precursors prior to publication. Thanks are also due to W. Horsthemke for valuable discussions. This work was supported in part by the British Science and Engineering Research Council, by a NATO Grant No. RG 85/0770 and by the U.S. Office of Naval Research Grant No. N00014-85-K-0372.

APPENDIX

A possible order parameter which could characterize the onset of limit-cycle behavior in the presence of noise has been offered by San Miguel and Chaturvedi:[33]

$$\eta = (x\dot{y} - y\dot{x}) \mid_{P_{\text{st,max}}} , \tag{A1}$$

that is, the circulation L_{xy} evaluated at the maximum of the stationary two-dimensional density. For a specific example they show that η becomes nonzero exactly at that point in parameter space for which the density undergoes a transition from a single-peaked shape, through which all cross sections perpendicular to the xy plane are also monomodal, to a (symmetric) crater shape with a closed rim (through which all vertical cross sections are bimodal). As indicated here by Figs. 4 and 5, the Brusselator densities, by contrast, pass through two transitions: (1) single peaked to craterlike but with a nonconnected rim and (2) nonconnected to connected rim. In the first case, a line joining all connected maxima does not close, while in the second case it does. Figure 10 shows sketches of such lines above horizontal cross sections of measured

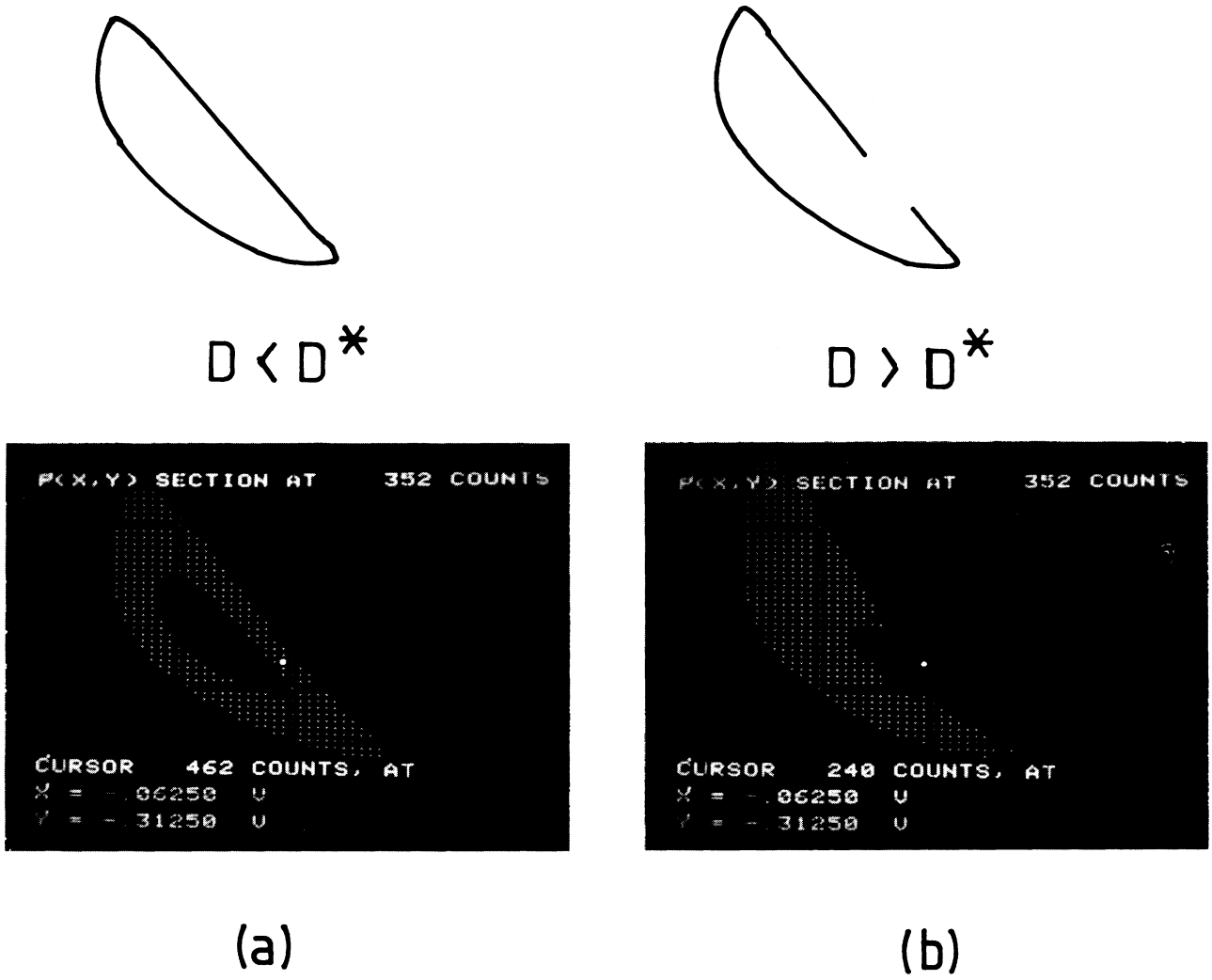

FIG. 10. Sketches of closed and open loci of connected maxima of the Brusselator stationary statistical densities, showing the two topologies: (a) horizontal cross sections above a certain altitude are doubly connected, and (b) all horizontal cross sections are singly connected. The photographs show examples of measured cross sections for $B > B_c$ at two values of D as indicated. The cursor (bright spot) marks the lowest altitude of the crater rim in (a), and marks the same location in (b) with D increased above D^*.

densities. Figure 10(a) shows a crater with a connected rim, where the cursor (bright spot) marks the point on the rim with the lowest altitude above the crater bottom. In Fig. 10(b) the noise intensity has been increased so that the bottom of the crater has risen above the rim and all horizontal cross sections are simply connected.

We have generalized the definition of the order parameter to include cases where there is a locus of connected maxima, not all at the same altitude (in contrast to the symmetric example given in Ref. 33):

$$\eta = \langle L_{xy} \rangle \mid_{\text{path}} = \int_{\text{path}} L_{xy}(s) ds \ , \tag{A2}$$

where "path" maps the locus of connected maxima as a function of s. Such paths may be expected to lie very close to those actual trajectories which occur with the highest probability. Though all physical trajectories must be closed, in order to preserve the topological differences indicated in Fig. 10, *we close the path integral in (A2) only when the locus of connected maxima is closed.* Using this definition, and Stokes' Theorem, it is straightforward to show that

$$\eta \propto A, \quad \text{for } B \geq B^* \text{ and } D \geq D^*$$
$$= 0, \quad \text{otherwise} \ , \tag{A3}$$

where A is the area enclosed by the path. In this way the order parameter proposed in Ref. 33 is reduced to a topological indicator which exactly identifies the critical density defined in the text of this paper.

We wish to remark that in this extended definition, η jumps discontinuously at the critical point. The physical significance of this jump is, however, doubtful since η is not a directly measurable quantity. It is the actual topology of the stationary density (which *is* a physical observable) which undergoes a drastic change at the critical point, in the Brusselator.

*Permanent address: Department of Physics, University of Missouri at St. Louis, St. Louis, MO 63121.

[1]R. Lefever and W. Horsthemke, Bull. Math. Biol. **41**, 469 (1979).
[2]R. Lefever and W. Horsthemke, Proc. Nat. Acad. Sci. U.S.A. **76**, 2490 (1979).
[3]A. Schenzle and H. Brand, Phys. Rev. A **20**, 1628 (1979).
[4]J. M. Sancho and M. San Miguel, Z. Phys. B **36**, 357 (1980).
[5]H. Fujisaka and S. Grossmann, Z. Phys. B **43**, 69 (1981).
[6]G. Welland and F. Moss, Phys. Lett. **89A**, 273 (1982).
[7]H. Brand and A. Schenzle, J. Phys. Soc. Jpn. **48**, 1382 (1980).
[8]F. Moss and G. Welland, Phys. Rev. A **25**, 3389 (1982).
[9]S. Kabashima and T. Kawakubo, Phys. Lett. **70A**, 375 (1979).
[10]S. D. Robinson, F. Moss, and P. V. E. McClintock, J. Phys. A **18**, L89 (1985).
[11]S. Kai, T. Kai, M. Takata, and K. Hisakawa, J. Phys. Soc. Jpn. **47**, 1379 (1979).
[12]T. Kawakubo, A. Yanagita, and S. Kabashima, J. Phys. Soc. Jpn. **50**, 1451 (1981).
[13]H. K. Brand, S. Kai, and S. Wakabayashi, Phys. Rev. Lett. **54**, 555 (1985).
[14]S. Kai, S. Wakabayashi, and M. Imasaki, Phys. Rev. A **33**, 2612 (1986).
[15]W. Horsthemke, C. R. Doering, R. Lefever, and A. S. Chi, Phys. Rev. A **31**, 1123 (1985).
[16]M. Lücke and F. Schank, Phys. Rev. Lett. **54**, 1465 (1985).
[17]G. Ahlers, P. C. Hohenberg, and M. Lucke, Phys. Rev. Lett. **53**, 48 (1984); Phys. Rev. A **32**, 3493 (1985).
[18]S. J. Linz and M. Lucke, Phys. Rev. A **33**, 2694 (1986).
[19]W. Horsthemke and R. Lefever, *Noise Induced Transitions: Theory and Applications in Physics, Chemistry and Biology* (Springer-Verlag, Berlin, 1984).
[20]C. R. Doering, Phys. Rev. A **34**, 2564 (1986).
[21]G. Broggi, A. Colombo, L. A. Lugiato, and P. Mandel, Phys. Rev. A **33**, 3635 (1986).
[22]R. Mannella, P. V. E. McClintock, and F. Moss, Phys. Rev. A **35**, 2560 (1987).
[23]R. Kapral and P. Mandel, Phys. Rev. A **32**, 1076 (1985).
[24]B. Morris and F. Moss, Phys. Lett. **118A**, 117 (1986).
[25]G. Nicolis and I. Prigogine, *Self-Organization in Nonequilibrium Systems* (Wiley, New York, 1977).
[26]R. Lefever and J. Wm. Turner, Phys. Rev. Lett. **56**, 1631 (1986).
[27]R. Graham, Phys. Rev. A **25**, 3234 (1982).
[28]E. Knobloch and K. A. Wiesenfeld, J. Stat. Phys. **33**, 611 (1983).
[29]P. Hanggi and P. Riseborough, Am. J. Phys. **51**, 347 (1983).
[30]K. Wiesenfeld, J. Stat. Phys. **38**, 1971 (1985).
[31]C. Jeffries and K. Wiesenfeld, Phys. Rev. A **31**, 1077 (1985).
[32]K. Wiesenfeld, Phys. Rev. A **32**, 1744 (1985).
[33]M. San Miguel and S. Chaturvedi, Z. Phys. B **40**, 167 (1980).
[34]K. Tomita, T. Todani, and H. Kidachi, Physica **A84**, 350 (1976), and references therein.
[35]Here $\langle V_n^2 \rangle = D/2\tau$, because of a difference in definition of the noise intensity between this work and that of LT.

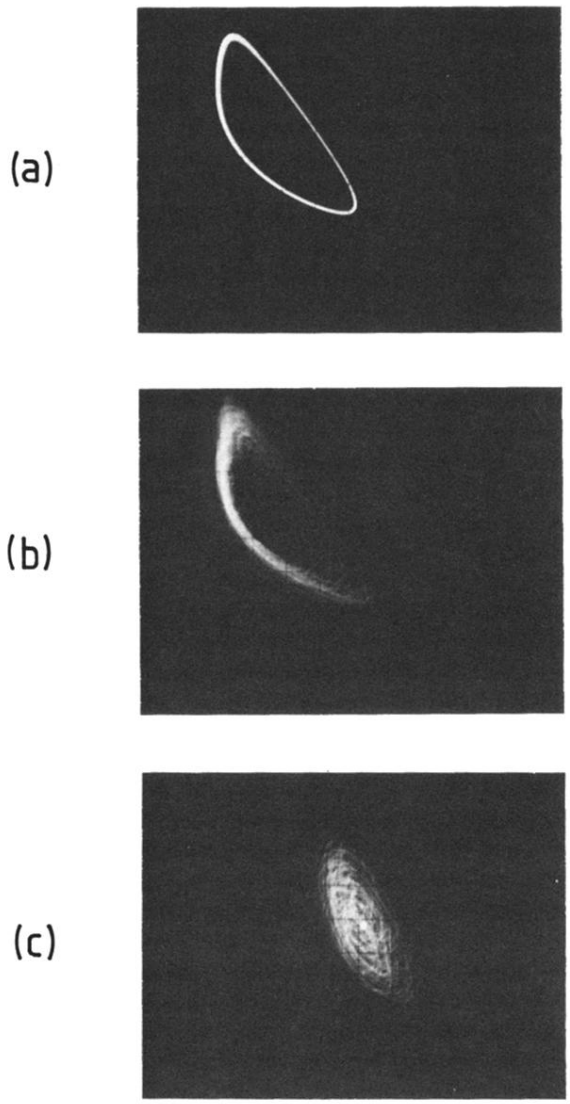

FIG. 1. Limit cycles y vs x of the electronic Brusselator. (a) for $B=2.5$ without external noise; (b) for $B=2.5$, $D=0.01$, and $\tau=0.10$, plotted on the same scale as (a); and (c) $B=1.8$ ($<B_c$), $D=0.01$, and $\tau=1.0$. The scale is expanded by a factor of 2.5 compared to (a) and (b). The dot at the center is the fixed point observed without external noise.

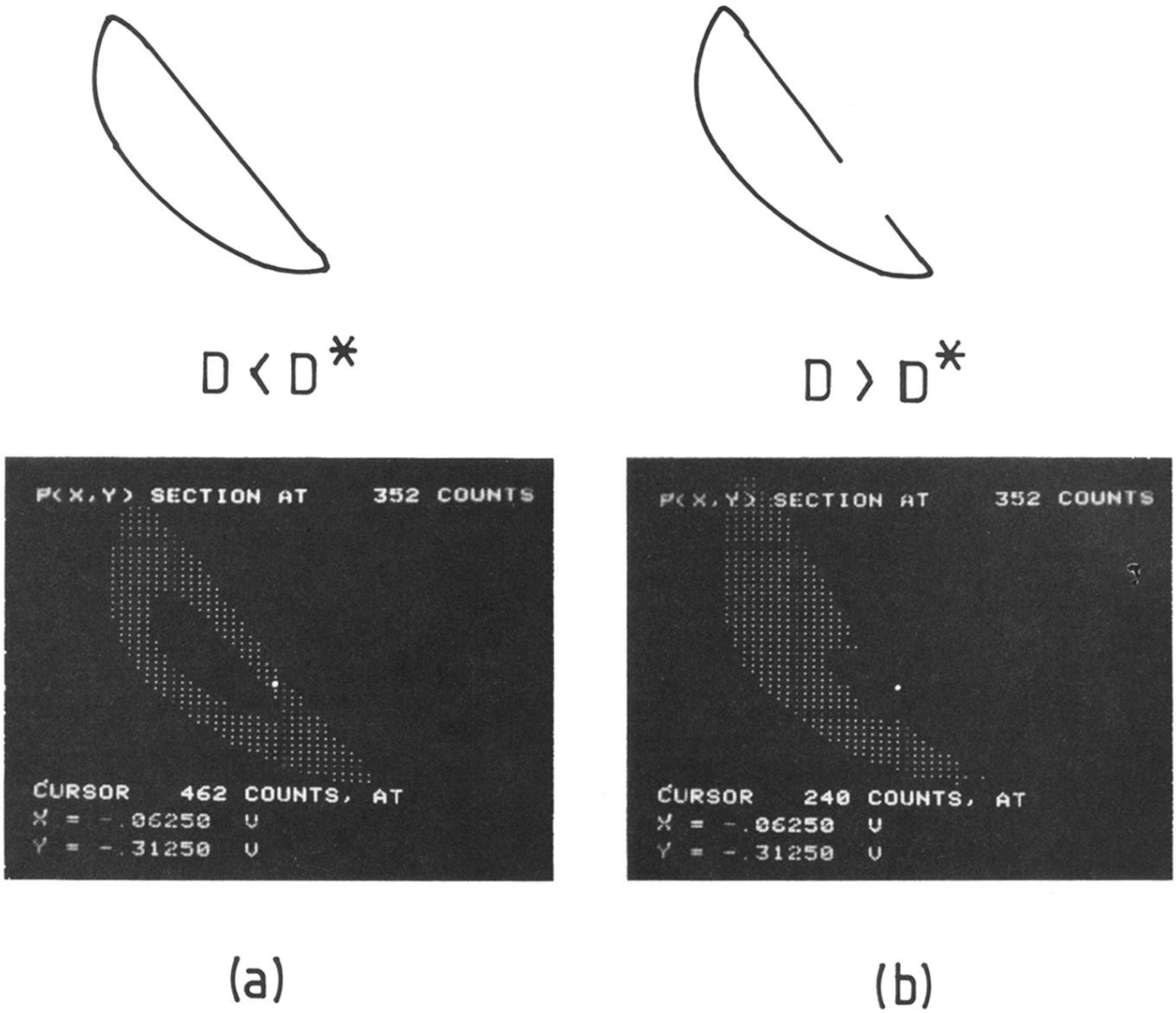

FIG. 10. Sketches of closed and open loci of connected maxima of the Brusselator stationary statistical densities, showing the two topologies: (a) horizontal cross sections above a certain altitude are doubly connected, and (b) all horizontal cross sections are singly connected. The photographs show examples of measured cross sections for $B > B_c$ at two values of D as indicated. The cursor (bright spot) marks the lowest altitude of the crater rim in (a), and marks the same location in (b) with D increased above D^*.